

Journal of Mechanics of Materials and Structures

**A FINITE ELEMENT FOR FORM-FINDING
AND STATIC ANALYSIS OF TENSEGRITY STRUCTURES**

Dario Gasparini, Katalin K. Klinka and Vinicius F. Arcaro

Volume 6, No. 9-10

November–December 2011

A FINITE ELEMENT FOR FORM-FINDING AND STATIC ANALYSIS OF TENSEGRITY STRUCTURES

DARIO GASPARINI, KATALIN K. KLINKA AND VINICIUS F. ARCARO

This text describes a mathematical model for both form-finding and static analysis of tensegrity structures. A special line element that shows constant stress for any displacement of its nodes is used to define a prestressed equilibrium configuration. The form-finding and static analysis are formulated as an unconstrained nonlinear programming problem, where the objective function is the total potential energy and the displacements of the nodal points are the unknowns. Analytical solutions for tensegrity prisms are presented and compared with the numerical results of the proposed approach. A quasi-Newton method is used, which avoids the evaluation of the tangent stiffness matrix. The source and executable computer codes of the algorithm are available for download from the website of one of the authors.

1. Introduction

A review of the important literature related to form-finding methods for tensegrity structures is given in [Tibert and Pellegrino 2003]. These methods can be classified into kinematical and statical methods. This text concentrates on the total potential energy minimization method for both form-finding and static analysis of tensegrity structures. A special line element that shows constant stress for any displacement of its nodes is used to define a prestressed equilibrium configuration. The form-finding and static analysis are formulated as an unconstrained nonlinear programming problem, where the objective function is the total potential energy and the displacements of the nodal points are the unknowns. A quasi-Newton method is used, which avoids the evaluation of the tangent stiffness matrix. There is an interesting connection between minimizing the total potential energy, which is defined by an unconstrained nonlinear programming problem, and the general method for form-finding first described in [Pellegrino 1986], which is defined by a constrained nonlinear programming problem. The strain energy for a line element can be interpreted as a penalty function, as it imposes resistance to changing the length of the element. Minimization methods based on penalty functions were the first methods used for constrained nonlinear programming. The total potential energy minimization method for the analysis of cable structures was first described in [Pietrzak 1978]. The following conventions apply unless otherwise specified or made clear by the context: a Greek letter expresses a scalar, and a lower-case letter represents a column vector.

2. Line element definition

Figure 1 shows the geometry of the element. The nodes are labeled 1 and 2. The nodal displacements transform the element from its initial configuration to its final configuration. The strain is assumed constant along the element and the material homogeneous and isotropic.

Keywords: cable, element, line, minimization, nonlinear, optimization, tensegrity.

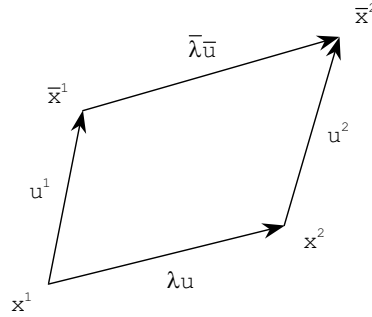


Figure 1. Line element.

3. Deformed length

The vector u is a unit vector. Note that λ represents the distance between the nodes of the element in this initial configuration. However, this distance will not always represent the undeformed length of the element. The nodal displacements vectors are numbered according to its node numbers. The deformed length can be written as

$$\bar{\lambda} = \lambda\sqrt{1 + \delta}, \tag{1}$$

where

$$\delta = 2u^T z + z^T z, \quad z = \frac{u^2 - u^1}{\lambda}. \tag{2}$$

The unit vector parallel to the element in its deformed configuration can be written as

$$\bar{u} = \frac{u + z}{\sqrt{1 + \delta}}. \tag{3}$$

4. State of constant cut

Consider an element with undeformed length less than the initial distance of its nodes. This situation can be pictured as an imaginary cut in the element's undeformed length. The element shows tension with zero nodal displacements. Considering μ as the value of the cut in the undeformed length, the strain-free length of the element can be written as

$$\rho = \frac{\mu}{\lambda}, \quad \lambda_0 = \lambda(1 - \rho). \tag{4}$$

The engineering strain can be written as

$$\varepsilon = \frac{\sqrt{1 + \delta} - 1 + \rho}{1 - \rho}. \tag{5}$$

Inaccuracy often results from the severe cancellation that occurs when nearly equal values are subtracted. In order to avoid it, the previous expression should be evaluated as

$$\varepsilon = \frac{\delta/(\sqrt{1 + \delta} + 1) + \rho}{1 - \rho}. \tag{6}$$

5. Potential strain energy

Considering σ as the conjugate stress to the engineering strain ε and α as the undeformed area of the element, the potential strain energy and its gradient with respect to the nodal displacements can be written as

$$\phi = \alpha \lambda_0 \int_0^\varepsilon \sigma(\xi) d\xi, \quad \frac{\partial \phi}{\partial u_i^1} = \alpha \lambda_0 \sigma(\varepsilon) \frac{\partial \varepsilon}{\partial u_i^1}, \quad \frac{\partial \phi}{\partial u_i^1} = -\alpha \sigma(\varepsilon) \bar{u}_i, \quad (7)$$

$$\frac{\partial \phi}{\partial u_i^2} = \alpha \lambda_0 \sigma(\varepsilon) \frac{\partial \varepsilon}{\partial u_i^2}, \quad \frac{\partial \phi}{\partial u_i^2} = +\alpha \sigma(\varepsilon) \bar{u}_i. \quad (8)$$

Note that the conjugate stress to the engineering strain is not the Cauchy stress. However, for practical purposes where the strain is usually small, this stress can be taken as an approximation to the Cauchy stress.

6. Geometric interpretation

Figure 2 shows the geometric interpretation of the gradient of the potential strain energy as forces acting on nodes of the element. These forces are known as internal forces.

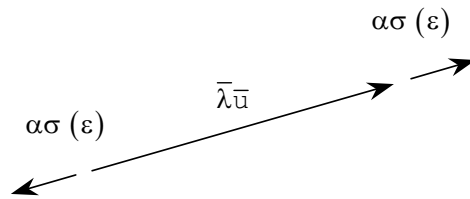


Figure 2. Geometric interpretation.

7. State of constant stress

Consider an element with strain-free length given by λ_0 . The engineering strain can be written as

$$\varepsilon = \frac{\bar{\lambda} - \lambda_0}{\lambda_0}. \quad (9)$$

Supposing that the element shows constant stress σ , the potential strain energy can be written as

$$\phi = \alpha \lambda_0 \int_0^\varepsilon \sigma d\xi = \alpha \sigma (\bar{\lambda} - \lambda_0). \quad (10)$$

The potential strain energy is equal to the force multiplied by the relative displacement between the nodes. In the expression for the strain energy, the strain-free length can be eliminated because it does not depend on the nodal displacements. Its permanence in the expression would only add constants, one for each element, to the total potential energy function. Minimizing a function plus a constant is equivalent to minimizing the function only. Therefore, the potential strain energy can be defined as

$$\phi = \alpha \sigma \lambda \sqrt{1 + \delta}. \quad (11)$$

The gradient with respect to the nodal displacements can be written as

$$\frac{\partial \varphi}{\partial u_i^1} = -\alpha \sigma \bar{u}_i, \quad \frac{\partial \varphi}{\partial u_i^2} = +\alpha \sigma \bar{u}_i. \quad (12)$$

The gradient can be interpreted as internal forces with constant modulus acting on nodes of the element. The element shows constant stress for any displacement of its nodes. A similar element was described in [Meek 1971]. The element was called a variable initial length element.

8. Internal forces equivalence

A cut value is equivalent to a stress value in the sense that they both produce the same internal forces. The following approach can be used when stress is a nonlinear invertible function of strain.

To find the cut value equivalent to the stress value, first find the strain:

$$\sigma(\varepsilon) = \sigma. \quad (13)$$

Then, find the cut value:

$$\mu = \frac{\lambda}{(1 + \varepsilon)} \left(\varepsilon - \frac{\delta}{1 + \sqrt{1 + \delta}} \right). \quad (14)$$

To find the stress value equivalent to the cut value, first find the strain:

$$\varepsilon = \frac{\delta / (\sqrt{1 + \delta} + 1) + \rho}{1 - \rho}. \quad (15)$$

Then, find the stress:

$$\sigma = \sigma(\varepsilon). \quad (16)$$

9. Stress and strain

For simplicity, consider a linear function with E as the modulus of elasticity. The potential strain energy can be written as

$$\sigma = E\varepsilon, \quad \varphi = \frac{1}{2} \alpha \lambda_0 E \varepsilon^2. \quad (17)$$

In the case of a hyperelastic material, it is important to emphasize that the strain energy and its corresponding Cauchy stress can be written as functions of the nodal displacements. Therefore, this type of material can be considered without introducing any additional difficulty.

10. Analysis strategy

The initial configuration of a tensegrity structure is defined as the configuration of zero nodal displacements for all its nodes. An analysis strategy can be defined as follows: Select some elements and set them to the constant stress state by specifying a stress value. Find the prestressed equilibrium configuration. At this equilibrium configuration, change the elements from the constant stress state to its equivalent constant cut state. Note that the equilibrium configuration remains the same. Apply the loading and find the final equilibrium configuration.

11. Equilibrium configuration

Considering u as the vector of unknown displacements and f as the vector of applied nodal forces, the total potential energy function and its gradient can be written as

$$\pi(u) = \sum_{\text{elements}} \varphi(u) - f^T u, \quad \nabla \pi(u) = \sum_{\text{elements}} \nabla \varphi(u) - f. \quad (18)$$

The stable equilibrium configurations correspond to local minimum points of the total potential energy function. In order to find the local minimum points of a nonlinear multivariate function, the general strategy that can be used is: Choose a starting point and move in a given direction such that the function decreases. Find the minimum point in this direction and use it as a new starting point. Continue this way until a local minimum point is reached. The problem of finding the minimum points of a nonlinear multivariate function is replaced by a sequence of subproblems, each one consisting of finding the minimum of a univariate nonlinear function. In the quasi-Newton methods, starting with the unit matrix, a positive-definite approximation to the inverse of the Hessian matrix is updated at each iteration. This update is made using only values of the gradient vector. A direction such that the function decreases is calculated as minus the product of this approximation of the inverse of the Hessian matrix and the gradient vector calculated at the starting point of each iteration. Consequently, it is not necessary to solve any system of equations. Moreover, analytical derivation of an expression for the Hessian matrix is not necessary. Note that by minimizing the total potential energy function it is almost impossible to find an unstable equilibrium configuration, which corresponds to a local maximum point. The only exception is that it is possible to find a saddle point, that is, a point that is a local minimum and also a local maximum. However, even in this improbable situation, a direction of negative curvature to continue toward a local minimum point can be found as described in [Gill and Murray 1974]. It is important to emphasize that minimizing total potential energy to find equilibrium configurations does not require support constraints to prevent rigid body motion. The computer code uses the limited-memory BFGS algorithm to tackle large-scale problems as described in [Nocedal and Wright 1999]. It also employs a line search procedure through cubic interpolation, as described in the same reference.

12. Geometrical shape minimization

Consider the following special case: A structure composed of elements in the state of constant stress with stress equal to one and elements in the state of constant cut with cut equal to zero. The area is equal to one for all elements. The vector of applied nodal forces is equal to zero. The stress-strain relationship is given by a linear function with E as the modulus of elasticity. The total potential energy can be written as

$$\pi(u) = \sum_{\text{stress}} \lambda \sqrt{1 + \delta} + \frac{E}{2} \sum_{\text{cut}} \lambda e^2. \quad (19)$$

The strain energy of an element in the state of constant stress is simply its final length. A high modulus of elasticity imposes resistance for changing the length of an element in the state of constant cut. The strain energy of an element in the state of constant cut can be interpreted as a penalty function. The problem can be interpreted as a constrained nonlinear programming problem of minimizing the sum of the lengths of the elements in the state of constant stress while keeping the lengths of the elements in the state of constant cut. This leads to an extension of the mathematical model of [Arcaro and Klinka 2009].

13. Analysis of a simple tensegrity

This problem and its relation to tensegrity structures was first described in [Calladine 1978]. Figure 3 shows a two-element truss with a vertical displacement on the center node.

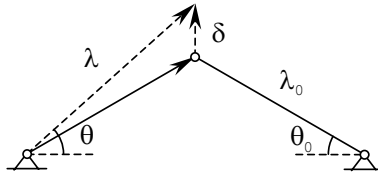


Figure 3. Two-element truss.

13.1. Geometry. From Figure 3 we can write

$$\lambda \cos \theta = \lambda_0 \cos \theta_0, \quad \lambda \sin \theta = \lambda_0 \sin \theta_0 + \delta. \quad (20)$$

13.2. Element length. The element length as function of the rotation angle can be written as

$$\lambda(\theta) = \frac{\lambda_0 \cos \theta_0}{\cos \theta}. \quad (21)$$

The derivative of the rotation angle with respect to the vertical displacement can be written as

$$\frac{d\theta}{d\delta} = \frac{\cos^2 \theta}{\lambda_0 \cos \theta_0}. \quad (22)$$

13.3. Equilibrium equation. Considering α as the undeformed area of the elements, the total potential strain energy can be written as

$$\varphi = 2\alpha\lambda_\mu \int_0^\varepsilon \sigma(\xi) d\xi. \quad (23)$$

The derivative of the total potential strain energy with respect to the vertical displacement is equal to the force applied in the direction of this displacement (note that the force is positive upward):

$$f = \frac{d\varphi}{d\varepsilon} \frac{d\varepsilon}{d\theta} \frac{d\theta}{d\delta}, \quad f = 2\alpha\sigma(\varepsilon) \frac{\cos^2 \theta}{\lambda_0 \cos \theta_0} \lambda'(\theta). \quad (24)$$

13.4. Element strain. Considering a cut μ in the initial length of the element, its undeformed length can be written as

$$\lambda_\mu = \lambda_0 - \mu. \quad (25)$$

The element strain can be written as

$$\varepsilon = \frac{\lambda(\theta)}{\lambda_\mu} - 1. \quad (26)$$

13.5. Stress and strain. The following approach can be used when stress is a nonlinear invertible function of strain. For simplicity, consider a linear function with E as the modulus of elasticity. By imposing a tension σ_μ on the elements at the prestressed configuration, its undeformed lengths can be written as

$$\lambda_\mu = \frac{\lambda_0 \cos \theta_0}{(1 + \sigma_\mu/E)}. \tag{27}$$

The cut in the initial length of the elements is given by

$$\mu = \lambda_0 - \lambda_\mu. \tag{28}$$

The equilibrium equation can be written as

$$\frac{f}{E\alpha} = 2 \sin \theta \left[\left(1 + \frac{\sigma_\mu}{E} \right) \frac{1}{\cos \theta} - 1 \right]. \tag{29}$$

Figure 4 shows the nondimensional force as a function of the rotation angle for $\sigma_\mu/E = 0.001$.

The axial force on the elements can be written as

$$\alpha \sigma(\varepsilon) = \alpha E \left[\left(1 + \frac{\sigma_\mu}{E} \right) \frac{1}{\cos \theta} - 1 \right]. \tag{30}$$

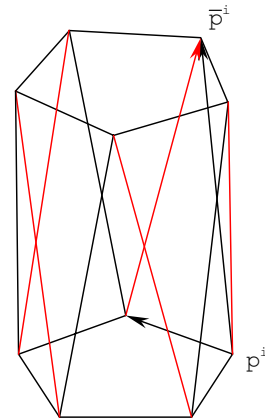
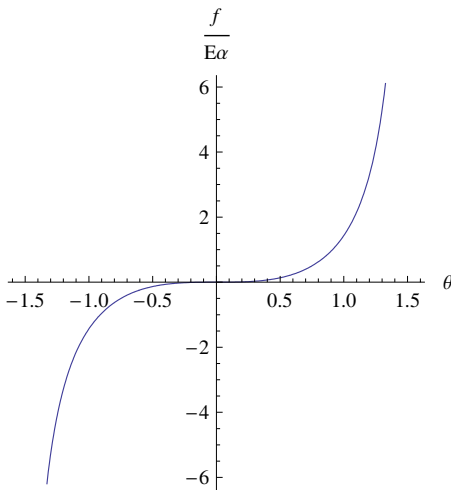


Figure 4. Nondimensional force versus rotation angle.

Figure 5. Straight tensegrity prism.

14. Analysis of tensegrity prisms

The analysis of [Oppenheim and Williams 2000] for a three-sided tensegrity prism is extended to a n -sided tensegrity prism. Figure 5 shows a straight tensegrity prism. The bottom and top regular polygons are inscribed in circles of equal radius. The sum of the lengths of the diagonal elements (shown in red) is minimized by rotating the top polygon counterclockwise with respect to the bottom polygon, while the lengths of the elements shown in black remain constant. The geometry defined by the final shape is also called a minimal tensegrity prism and can be used as a building block of complex tensegrity structures [Skelton and de Oliveira 2009].

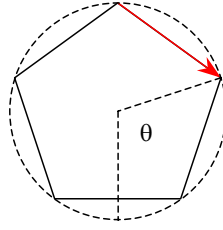


Figure 6. Top view of a straight tensegrity prism.

14.1. Geometry. For n -sided regular polygons, the coordinates of the vertices can be written as

$$\gamma = \frac{2\pi}{n}, \quad p^i = \begin{bmatrix} \rho \cos(\gamma i) \\ \rho \sin(\gamma i) \\ 0 \end{bmatrix}, \quad \bar{p}^i = \begin{bmatrix} \rho \cos(\theta + \gamma i) \\ \rho \sin(\theta + \gamma i) \\ \delta(\theta) \end{bmatrix}. \quad (31)$$

The following vectors are defined in terms of the coordinates of the vertices:

$$b^i = p^{i+1} - p^i, \quad l^i = \bar{p}^i - p^{i+1}, \quad v^i = \bar{p}^i - p^i. \quad (32)$$

14.2. Interval for the rotation angle. Figure 6 shows the top view of a straight tensegrity prism with one diagonal element shown in red.

The maximum clockwise rotation happens when a diagonal element intercepts the vertical axis on the center of the circle resulting in diagonal elements interference. This rotation angle is given by

$$\theta_{\min} = -(\pi - \gamma). \quad (33)$$

The maximum counterclockwise rotation happens when a vertical element (connects corresponding vertices of top and bottom polygons) intercepts the vertical axis on the center of the circle resulting in vertical elements interference. This rotation angle is given by

$$\theta_{\max} = \pi. \quad (34)$$

The interval for the rotation angle is

$$-(\pi - \gamma) \leq \theta \leq \pi. \quad (35)$$

14.3. Height. The square of the norm of vector v^i can be written as

$$\|v^i\|^2 = 2\rho^2(1 - \cos \theta) + \delta^2(\theta). \quad (36)$$

Considering v as the norm of vector v^i , which is constant, the expression for the height as function of rotation angle can be written as

$$\delta^2(\theta) = v^2 - 2\rho^2(1 - \cos \theta). \quad (37)$$

14.4. Diagonal element length. Considering λ as the norm of vector l^i , the square of the diagonal element length can be written as

$$\lambda^2(\theta) = v^2 + 2\rho^2[\cos \theta - \cos(\theta - \gamma)]. \quad (38)$$

14.5. Minimum diagonal element length. Due to symmetry, minimizing the sum of the diagonal element lengths is equivalent to minimizing the square of one diagonal element length.

$$\frac{\partial \lambda^2}{\partial \theta} = 0 \quad \Rightarrow \quad \tan \bar{\theta} = \frac{\sin \gamma}{\cos \gamma - 1}. \quad (39)$$

Notice that this expression is valid when the diagonal elements connect the corresponding bottom and top points in any symmetric way:

$$\bar{\theta} > 0 \quad \Rightarrow \quad \cos \bar{\theta} = \frac{\cos \gamma - 1}{\sqrt{2(1 - \cos \gamma)}}, \quad (40)$$

$$\bar{\theta} > 0 \quad \Rightarrow \quad \sin \bar{\theta} = \frac{\sin \gamma}{\sqrt{2(1 - \cos \gamma)}}. \quad (41)$$

14.6. Element strain. Considering a cut μ in the initial length of the diagonal element, its undeformed length can be written as

$$\lambda_\mu = \lambda(0) - \mu. \quad (42)$$

The element strain can be written as

$$\varepsilon = \frac{\lambda(\theta)}{\lambda_\mu} - 1. \quad (43)$$

14.7. Equilibrium equation. Considering α as the undeformed area of the diagonal elements, the total potential strain energy can be written as

$$\varphi = n\alpha\lambda_\mu \int_0^\varepsilon \sigma(\xi) d\xi. \quad (44)$$

The derivative of the total potential strain energy with respect to the vertical displacement is equal to the force applied in the direction of this displacement. This derivative is equal to the derivative with respect to the height (note that the force is positive upward when the vertical displacements of the bottom vertices are fixed):

$$f = \frac{d\varphi}{d\varepsilon} \frac{d\varepsilon}{d\theta} \frac{d\theta}{d\delta}, \quad f = n\alpha\sigma(\varepsilon) \left[1 - \frac{\sin(\theta - \gamma)}{\sin \theta} \right] \frac{\delta(\theta)}{\lambda(\theta)}. \quad (45)$$

14.8. Stress and strain. The following approach can be used when stress is a nonlinear invertible function of strain. For simplicity, consider a linear function with E as the modulus of elasticity. By imposing a tension σ_μ on the diagonal elements at the prestressed configuration, its undeformed lengths can be written as

$$\lambda_\mu = \frac{\sqrt{v^2 - 2\rho^2 \sqrt{2(1 - \cos \gamma)}}}{(1 + \sigma_\mu/E)}. \quad (46)$$

The cut in the initial length of the diagonal elements can be written as

$$\mu = \lambda(0) - \lambda_\mu. \quad (47)$$

The equilibrium equation can be written as

$$\frac{f}{E\alpha} = n \left[\frac{1}{\lambda_\mu} - \frac{1}{\lambda(\theta)} \right] \left[1 - \frac{\sin(\theta - \gamma)}{\sin \theta} \right] \delta(\theta). \quad (48)$$

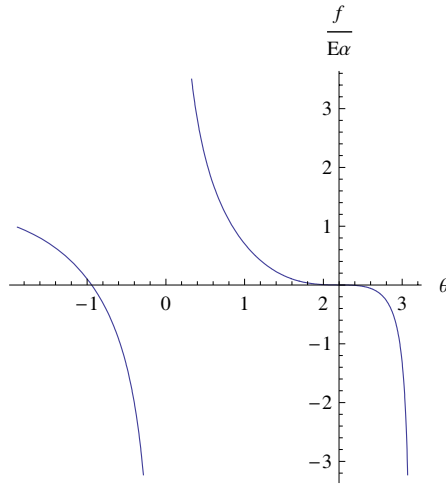


Figure 7. Nondimensional force versus rotation angle.

Figure 7 shows the nondimensional force as a function of the rotation angle for $n = 5$, $\nu/\rho = 3$, and $\sigma_\mu/E = 0.001$. Note that the vertical axis is placed on the position defined by the prestressed configuration.

The axial force on the diagonal elements can be written as $\alpha\sigma(\varepsilon) = \alpha E \left[\frac{\lambda(\theta)}{\lambda_\mu} - 1 \right]$.

15. The stella octangula

Figure 8 shows the geometry of a sculpture called the stella octangula, which was proposed by the Hungarian architect, sculptor and author David Georges Emmerich. An extensive description of his works is given in [Chassagnoux 2006]. An analysis of this structure, using the dynamic relaxation method, was given in [Motro 2011].

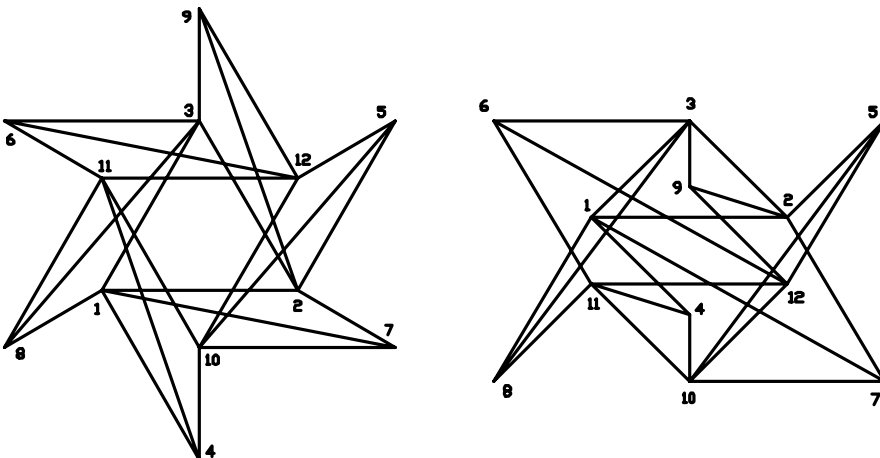


Figure 8. The stella octangula.

The geometry is composed of 18 elements with length s and 6 diagonal elements with length $s\sqrt{3}$. The diagonal elements are connected as follows:

| Element | Node | Node |
|---------|------|------|
| 3 | 4 | 11 |
| 6 | 5 | 10 |
| 9 | 6 | 12 |
| 12 | 7 | 1 |
| 15 | 8 | 3 |
| 18 | 9 | 2 |

Next we give the coordinates of the vertices, in terms of the parameters $r = s/\sqrt{3}$ and $h = s/\sqrt{6}$:

| Node | X | Y | Z | Node | X | Y | Z |
|------|--------|--------|-----|------|--------|-------|------|
| 1 | $-s/2$ | $-r/2$ | h | 7 | s | $-r$ | $-h$ |
| 2 | $s/2$ | $-r/2$ | h | 8 | $-s$ | $-r$ | $-h$ |
| 3 | 0 | r | h | 9 | 0 | $2r$ | $-h$ |
| 4 | 0 | $-2r$ | h | 10 | 0 | $-r$ | $-h$ |
| 5 | s | r | h | 11 | $-s/2$ | $r/2$ | $-h$ |
| 6 | $-s$ | r | h | 12 | $s/2$ | $r/2$ | $-h$ |

16. Examples

In the illustrations given in this section, elements shown in red are in compression; elements shown in blue are in tension; and elements in the initial configuration that start in the state of constant stress are shown in green.

Example 16.1 (A two-element truss with a vertical downward force applied on the center node). The force was calculated to make the element rotate -45 degrees from the prestressed configuration. The analytical expression for the equilibrium equation is presented in Section 12. The parameter values are

$$\theta_0 = 45 \text{ degrees}, \quad \lambda_0 = 1, \quad E = 1000, \quad \alpha = 1, \quad \sigma_\mu = 1, \quad f = -587.7864.$$

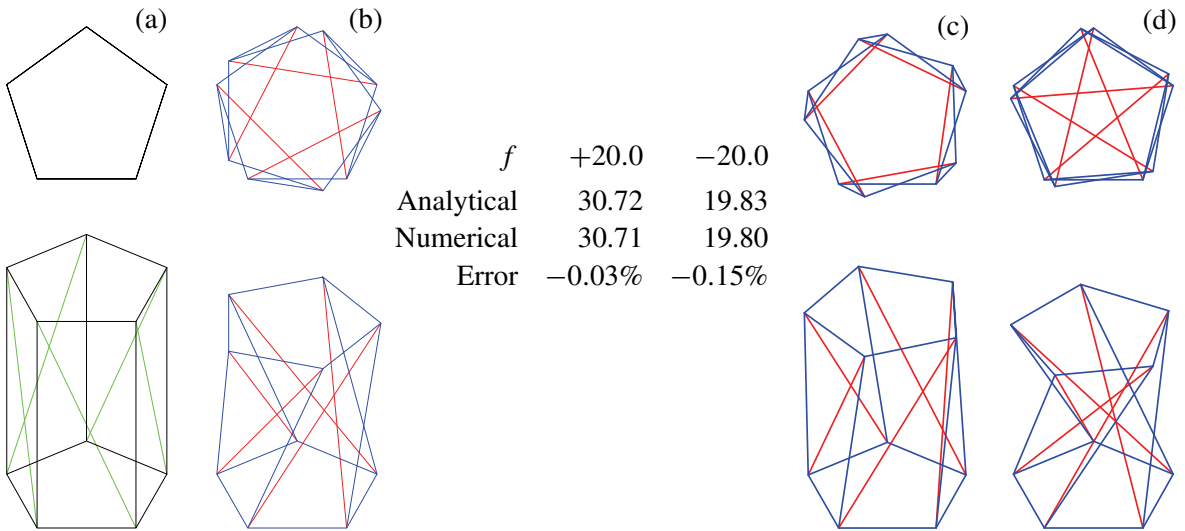
The value of the axial force found numerically coincides with the analytic one: 415.6278.

Here are the initial (left), prestressed (middle) configurations, and loaded (right) configurations:



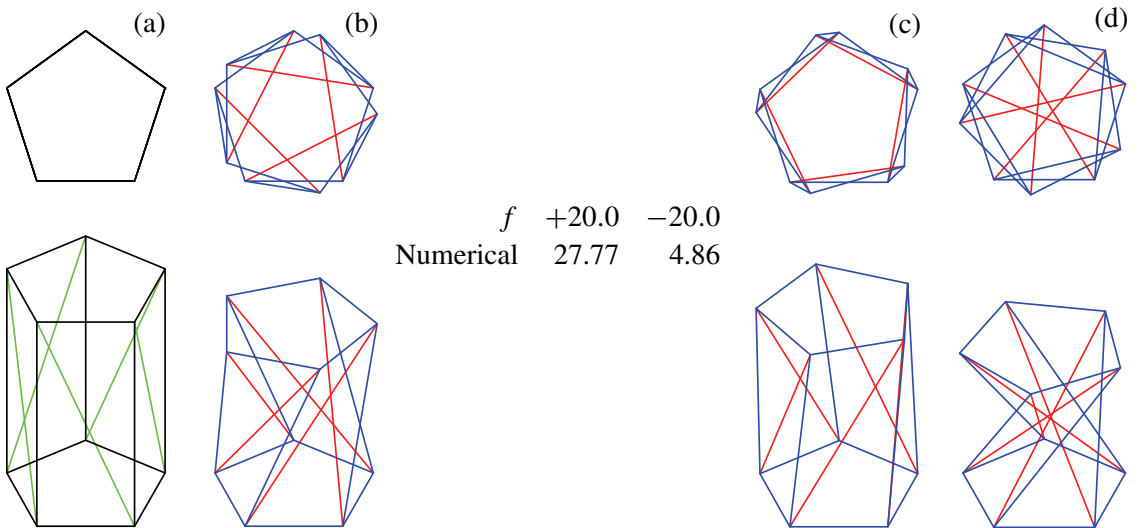
Example 16.2 (A pentagonal prism with vertical forces applied on the top nodes). The bottom nodes are fixed only in the vertical direction. The analytical expression for the equilibrium equation is presented in Section 13. The parameter values are $n = 5$, $\nu = 3$, $\rho = 1$, $E = 1000$ for the diagonal elements, $E = 1000000$ to simulate the inextensible elements, $\alpha = 1$, and $\sigma_\mu = 1$.

Here are the initial (a) and the prestressed (b) configurations; the rotation angle from the initial configuration is equal to 126 degrees.



Also shown in (c) is the loaded configuration for $f = 20$ (rotation angle of about -34 degrees from the prestressed configuration), and in (d) the loaded configurations for $f = -20$ (rotation angle of about 27 degrees). The values for the axial force on the diagonal elements are given for these two cases.

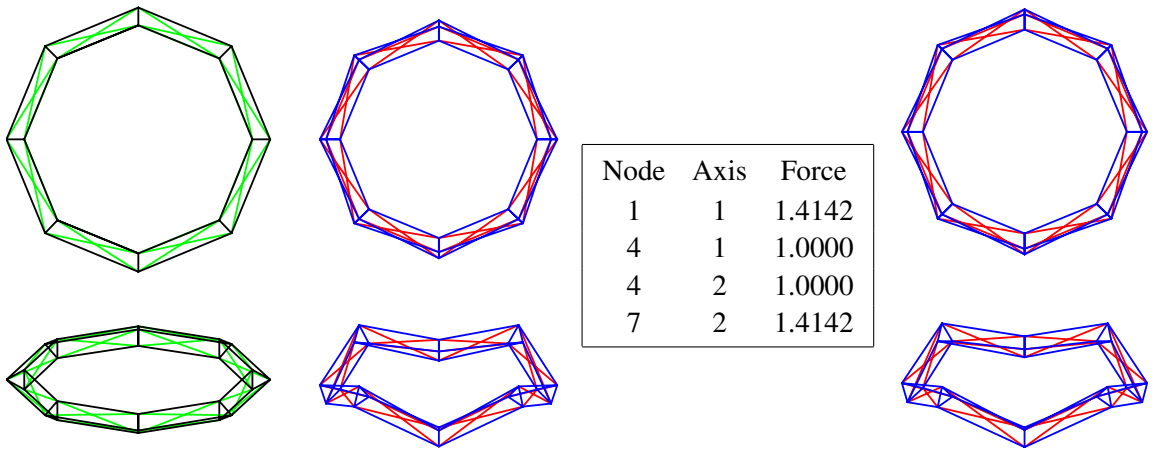
Example 16.3. This is the same structure described in [Example 16.2](#), except that $E = 1000$ for all elements. Here are the initial (a) and prestressed (b) configurations; the rotation angle from the initial configuration is 126 degrees.



Also shown in (c) is the loaded configuration for $f = 20$ (rotation angle of about -38 degrees from the prestressed configuration), and in (d) the loaded configurations for $f = -20$ (rotation angle of about 45 degrees). The values for the axial force on the diagonal elements are given for these two cases.

Example 16.4 (A circular prism with axis on a circumference of radius 10). The section is defined by a regular triangle inscribed in a circle of radius 1. It is composed of 72 elements. The modulus of elasticity is 1000. The elements have area 1. Note that this is a nonplanar circular tensegrity that originates from connecting the ends of a straight prism tensegrity. This is a simple idea that can be used to define circular nonplanar tensegrities with any number of segments. A circular planar tensegrity was described recently in [Yuan et al. 2008]. Elements in the initial configuration that start in the state of constant stress are shown in green with stress of 5. There are no support constraints. The loading consists of self-equilibrated radial forces applied on the nodes of the exterior circumference.

Here are the initial (left), prestressed (middle), and loaded (right) configurations under the forces shown in the table.



The elements are connected as follows:

| | | | | | | | | | | | | | | | | | | | | | |
|---------|---|---|---|---|---|---|---|---|---|----|----|----|----|----|----|----|----|----|----|----|----|
| Element | 1 | 2 | 3 | 4 | 5 | 6 | 7 | 8 | 9 | 25 | 26 | 27 | 28 | 29 | 30 | 49 | 50 | 51 | 52 | 53 | 54 |
| Node | 1 | 2 | 3 | 4 | 5 | 6 | 7 | 8 | 9 | 1 | 2 | 3 | 5 | 6 | 4 | 2 | 3 | 1 | 4 | 5 | 6 |
| Node | 2 | 3 | 1 | 5 | 6 | 4 | 8 | 9 | 7 | 4 | 5 | 6 | 8 | 9 | 7 | 4 | 5 | 6 | 8 | 9 | 7 |

Here are the coordinates of the initial (left), prestressed (middle), and loaded (right) configurations. Due to symmetry, the tables show information for only one fourth of the structure.

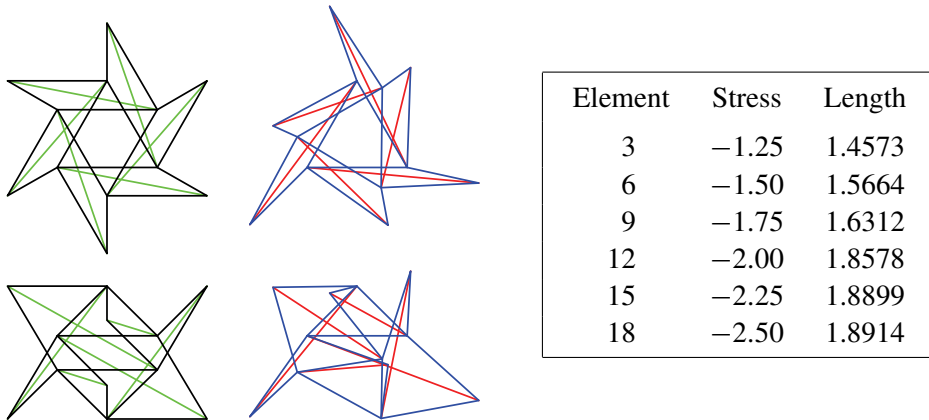
| | | | | | | | | | | | |
|------|---------|---------|---------|------|---------|---------|---------|------|---------|---------|---------|
| Node | X | Y | Z | Node | X | Y | Z | Node | X | Y | Z |
| 1 | 11.0000 | 0.0000 | 0.0000 | 1 | 9.3879 | -0.0000 | -2.1490 | 1 | 9.5010 | -0.0000 | -2.0677 |
| 2 | 9.5000 | 0.0000 | 0.8660 | 2 | 9.9007 | 0.0000 | -0.4922 | 2 | 9.9371 | 0.0000 | -0.3904 |
| 3 | 9.5000 | 0.0000 | -0.8660 | 3 | 8.2098 | 0.0000 | -0.8759 | 3 | 8.2630 | 0.0000 | -0.8446 |
| 4 | 7.7782 | 7.7782 | 0.0000 | 4 | 6.6382 | 6.6382 | 2.1490 | 4 | 6.7182 | 6.7182 | 2.0677 |
| 5 | 6.7175 | 6.7175 | 0.8660 | 5 | 5.8052 | 5.8052 | 0.8759 | 5 | 5.8428 | 5.8428 | 0.8446 |
| 6 | 6.7175 | 6.7175 | -0.8660 | 6 | 7.0009 | 7.0009 | 0.4922 | 6 | 7.0266 | 7.0266 | 0.3904 |
| 7 | 0.0000 | 11.0000 | 0.0000 | 7 | 0.0000 | 9.3879 | -2.1490 | 7 | 0.0000 | 9.5010 | -2.0677 |
| 8 | 0.0000 | 9.5000 | 0.8660 | 8 | -0.0000 | 9.9007 | -0.4922 | 8 | -0.0000 | 9.9371 | -0.3904 |
| 9 | 0.0000 | 9.5000 | -0.8660 | 9 | 0.0000 | 8.2098 | -0.8759 | 9 | 0.0000 | 8.2630 | -0.8446 |

The next table shows the axial force for the prestressed and the loaded configurations:

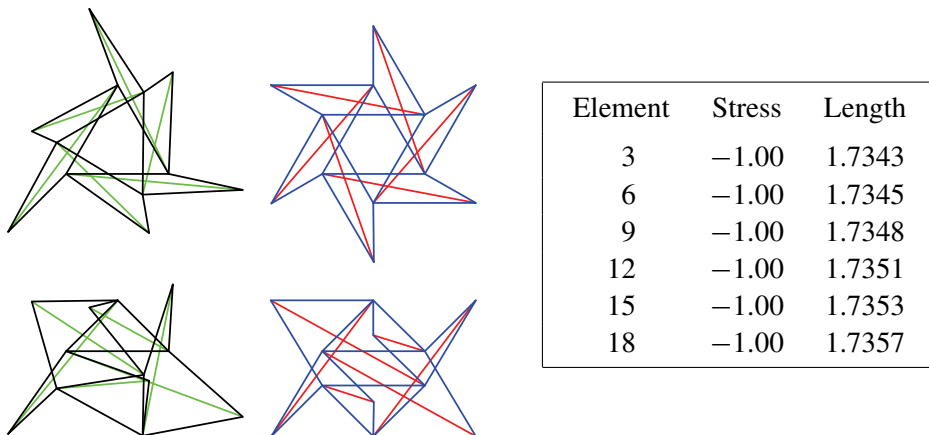
| | | | | | | | |
|---------|---------|---------|---------|---------|----------------|----------------|--------|
| Element | 1, 6, 7 | 2, 5, 8 | 3, 4, 9 | 25, 30 | 26, 27, 28, 29 | 49, 51, 52, 54 | 50, 53 |
| Force | 1.3113 | 1.0841 | 1.4375 | -5.5232 | -4.9454 | 5.0000 | 5.0000 |
| Force | 0.5762 | 1.5137 | 4.7852 | -6.3702 | -4.1728 | 3.7936 | 8.5064 |

Example 16.5 (A stella octangula with parameter $s = 1$). The modulus of elasticity is 1000. The elements have area 1. There are support constraints on nodes 1, 2, and 3 to prevent rigid body motion. A nonregular tensegrity can be generated by imposing different stress values for selected elements of a regular tensegrity. The regular tensegrity can be recovered by imposing equal stress values for the same selected elements on the previously generated nonregular tensegrity.

We illustrate here the initial configuration of the regular stella octangula and its prestressed configuration (nonregular stella octangula). The stress values for the diagonal elements of the initial configuration and the lengths of the diagonal elements of the prestressed configuration are also shown.



Finally, we illustrate the initial configuration of the nonregular stella octangula and its prestressed version, which is again a regular stella octangula. The stress values for the diagonal elements (initial configuration) and the lengths of the diagonal elements (prestressed configuration) are also shown.



17. Conclusions

A mathematical model is presented for form-finding and static analysis of tensegrity structures. The proposed model shows good agreement with analytical solutions for regular tensegrity structures. It can also handle nonregular tensegrity structures. The minimization of total potential energy has several advantages over solving the equilibrium equations in nonlinear mechanics: it allows solving for under-constrained structures. It is not necessary to derive the tangent stiffness matrix. It is not necessary to solve any system of equations. The model can handle large-scale problems.

References

- [Arcaro and Klinka 2009] V. F. Arcaro and K. K. Klinka, “Finite element analysis for geometrical shape minimization”, *J. Int. Assoc. Shell Spat. Struct.* **50**:2 (2009), 79–86.
- [Calladine 1978] C. R. Calladine, “Buckminster Fuller’s “Tensegrity” structures and Clerk Maxwell’s rules for the construction of stiff frames”, *Int. J. Solids Struct.* **14**:2 (1978), 161–172.
- [Chassagnoux 2006] A. Chassagnoux, “David Georges Emmerich: Professor of morphology”, *Int. J. Space Struct.* **21**:1 (2006), 59–71.
- [Gill and Murray 1974] P. E. Gill and W. Murray, “Newton-type methods for unconstrained and linearly constrained optimization”, *Math. Program.* **7**:1 (1974), 311–350.
- [Meek 1971] J. L. Meek, *Matrix structural analysis*, McGraw-Hill, New York, 1971.
- [Motro 2011] R. Motro, “Structural morphology of tensegrity systems”, *Meccanica* **46**:1 (2011), 27–40.
- [Nocedal and Wright 1999] J. Nocedal and S. J. Wright, *Numerical optimization*, Springer, New York, 1999.
- [Oppenheim and Williams 2000] I. J. Oppenheim and W. O. Williams, “Geometric effects in an elastic tensegrity structure”, *J. Elasticity* **59**:1-3 (2000), 51–65.
- [Pellegrino 1986] S. Pellegrino, *Mechanics of kinematically indeterminate structures*, Ph.D. thesis, University of Cambridge, 1986.
- [Pietrzak 1978] J. Pietrzak, “Matrix formulation of static analysis of cable structures”, *Comput. Struct.* **9**:1 (1978), 39–42.
- [Skelton and de Oliveira 2009] R. E. Skelton and M. C. de Oliveira, *Tensegrity systems*, Springer, New York, 2009.
- [Tibert and Pellegrino 2003] A. G. Tibert and S. Pellegrino, “Review of form-finding methods for tensegrity structures”, *Int. J. Space Struct.* **18**:4 (2003), 209–223.
- [Yuan et al. 2008] X. Yuan, Z. Peng, S. Dong, and B. Zhao, “A new tensegrity module: “torus””, *Adv. Struct. Eng.* **11**:3 (2008), 243–251.

Received 4 Aug 2010. Revised 10 Jan 2011. Accepted 5 Feb 2011.

DARIO GASPARINI: dag6@cwru.edu

Civil Engineering Department, Case Western Reserve University, 2182 Adelbert Road, Cleveland, OH 44106-7201, United States

KATALIN K. KLINKA: katalin@klinka.hu

Department of Structural Engineering, Budapest University of Technology and Economics, 2 Bertalan Lajos, Budapest H-1111, Hungary

VINICIUS F. ARCARO: vinicius.arcaro@gmail.com

College of Civil Engineering, University of Campinas, Avenida Albert Einstein 951, Campinas, SP 13083-852, Brazil
<http://www.arcaro.org>

JOURNAL OF MECHANICS OF MATERIALS AND STRUCTURES

jomms.org

Founded by Charles R. Steele and Marie-Louise Steele

EDITORS

CHARLES R. STEELE Stanford University, USA
DAVIDE BIGONI University of Trento, Italy
IWONA JASIUK University of Illinois at Urbana-Champaign, USA
YASUHIRO SHINDO Tohoku University, Japan

EDITORIAL BOARD

H. D. BUI École Polytechnique, France
J. P. CARTER University of Sydney, Australia
R. M. CHRISTENSEN Stanford University, USA
G. M. L. GLADWELL University of Waterloo, Canada
D. H. HODGES Georgia Institute of Technology, USA
J. HUTCHINSON Harvard University, USA
C. HWU National Cheng Kung University, Taiwan
B. L. KARIHALOO University of Wales, UK
Y. Y. KIM Seoul National University, Republic of Korea
Z. MROZ Academy of Science, Poland
D. PAMPLONA Universidade Católica do Rio de Janeiro, Brazil
M. B. RUBIN Technion, Haifa, Israel
A. N. SHUPIKOV Ukrainian Academy of Sciences, Ukraine
T. TARNAI University Budapest, Hungary
F. Y. M. WAN University of California, Irvine, USA
P. WRIGGERS Universität Hannover, Germany
W. YANG Tsinghua University, China
F. ZIEGLER Technische Universität Wien, Austria

PRODUCTION contact@msp.org

SILVIO LEVY Scientific Editor

Cover design: Alex Scorpan

Cover photo: Mando Gomez, www.mandolux.com

See <http://jomms.org> for submission guidelines.

JoMMS (ISSN 1559-3959) is published in 10 issues a year. The subscription price for 2011 is US \$520/year for the electronic version, and \$690/year (+ \$60 shipping outside the US) for print and electronic. Subscriptions, requests for back issues, and changes of address should be sent to Mathematical Sciences Publishers, Department of Mathematics, University of California, Berkeley, CA 94720–3840.

JoMMS peer-review and production is managed by EditFLOW[®] from Mathematical Sciences Publishers.

PUBLISHED BY
 **mathematical sciences publishers**
<http://msp.org/>

A NON-PROFIT CORPORATION

Typeset in L^AT_EX

Copyright ©2011 by Mathematical Sciences Publishers

Journal of Mechanics of Materials and Structures

Volume 6, No. 9-10

November–December 2011

- Turtle shell and mammal skull resistance to fracture due to predator bites and ground impact** **DAVID L. HU, KELLY SIELERT and MICHAEL GORDON** 1197
- Linear buckling analysis of cracked plates by SFEM and XFEM** **P. M. BAIZ, S. NATARAJAN, S. P. A. BORDAS, P. KERFRIDEN and T. RABCZUK** 1213
- A finite element for form-finding and static analysis of tensegrity structures**
DARIO GASPARINI, KATALIN K. KLINKA and VINICIUS F. ARCARO 1239
- Structural design of pyramidal truss core sandwich beams loaded in 3-point bending** **MING LI, LINZHI WU, LI MA, BING WANG and ZHENGXI GUAN** 1255
- Wave scattering from a rectangular crack in an anisotropic cladding**
PER-ÅKE JANSSON 1267
- Effect of adding crumb tire rubber particles on the mechanical properties of DCPD-modified sulfur polymer mortars**
HAMED MARAGHECHI, IMAN FOTOVAT AHMADI and SIAMAK MOTAHARI 1283
- Uniqueness theorems in the equilibrium theory of thermoelasticity with microtemperatures for microstretch solids**
ANTONIO SCALIA and MERAB SVANADZE 1295
- Implications of shakedown for design of actively cooled thermostructural panels**
NATASHA VERMAAK, LORENZO VALDEVIT, ANTHONY G. EVANS, FRANK W. ZOK and ROBERT M. MCMEEKING 1313